

## Effect of surface and bulk pinning on the distribution of transport current in a superconducting film

L. Burlachkov

*Institute of Superconductivity, Department of Physics, Bar-Ilan University, Ramat-Gan 52900, Israel*

V. Ginodman and I. Shlimak

*Jack and Pearl Resnik Institute of Advanced Technology, Department of Physics, Bar-Ilan University, Ramat-Gan 52900, Israel*

(Received 22 May 1998)

We show, both experimentally and theoretically, that the inhomogeneous distribution of transport current produced by two contacts located at the opposite corners of a square film is significantly changed as the film becomes superconducting (the total current  $I$  flowing through the sample is kept constant). We analyze two possible sources for such a redistribution of transport current: (1) the nonlinear dependence of the resistivity  $\rho$  on the current density  $j$ , and (2) the effect of surface barriers. In our geometry these sources have the opposite effect and compete with each other. This technique can be easily modified for various sample and contact geometries and is useful for the analysis of pinning and creep of vortices in superconductors.

[S0163-1829(99)06213-X]

### I. INTRODUCTION

The interplay between the bulk pinning and surface barriers in high- $T_c$  superconductors (HTSC), which together determine the vortex motion and, in turn, voltage and energy dissipation, has been intensively explored during last years. This study includes magnetization<sup>1</sup> and transport<sup>2</sup> experiments, as well as numerous theoretical analyses.<sup>3,4</sup> The surface barriers can be divided into two major types: the Bean-Livingston surface barrier<sup>5</sup> and the geometrical barrier.<sup>6</sup> It has been proved that both of them play an important role in magnetic irreversibility of HTSC and dominate over the bulk pinning under certain conditions, especially in clean crystals at high temperatures ( $T_c - T \ll T_c$ ).

At the same time significant attention was focused on another basic problem: the strongly nonlinear dependence of the bulk activation energy  $U_{bulk}$  on the current density  $j$  and its divergence at small  $j$  as  $U_{bulk} \propto j^{-\mu}$ , as predicted by the collective creep theory.<sup>7,8</sup> This in turn results in a non-Ohmic resistivity  $\rho(j) \propto \exp(-U_{bulk}(j)/kT)$ . The exponent  $\mu$  discriminates between various creep regimes,<sup>8</sup> and its knowledge is very important<sup>8-10</sup> for identification of the vortex state.

We present a very simple method of local potential probing in transport measurements, which is useful for study of interplay between surface and bulk properties, as well as of the non-Ohmic behavior of  $\rho(j)$  in the bulk. To the best of our knowledge, such a method has not been applied to superconductors so far. In contrast with the classic four-contact experimental scheme, where the current is supposed to flow homogeneously (i.e.,  $\mathbf{j} = \text{const}$ ), our method is based on the *inhomogeneity of current distribution* in the sample. There are three sources for such an inhomogeneity: (i) the geometry of the sample and of the contacts; (ii) the dependence of the local resistance  $\rho$  on  $j$ , which can be very strong and nonlinear in the mixed state of superconductor due to exponential dependence  $\rho = \rho_0 \exp(-U_{bulk}(j)/kT)$ ; (iii) splitting of

the total current  $I$  into two components:  $I_{edge}$  flowing along the edge surfaces of the sample, and  $I_{bulk} = \int j ds$  flowing in the bulk (here  $s$  is the cross section of the sample).

We use one pair of pointlike current contacts which produces a nonhomogeneous current distribution even in the normal state, and two pairs of voltage contacts (in general one can use many such pairs within the framework of this method) measuring voltage at different locations over the sample. The weak dependence of  $\rho_n$  on  $j$  in the normal state can be neglected if compared to a very strong exponential dependence  $\rho(j)$  in the superconducting state. The surface barrier is absent in the normal state, i.e.,  $I_{edge} = 0$ . Thus the current distribution  $j$  and electrostatic potential  $\varphi$  can be found from the solution of a standard Laplace problem. The ratio of voltages measured in the normal state by different pairs of voltage contact should be independent of the total current  $I$  flowing across the sample and of the applied magnetic field  $B$  (except for the cases of prominent magnetoresistance). Such a ratio depends only on the geometry of the sample and on both current and voltage contact locations. As temperature or field are reduced, the sample becomes superconducting, and its resistivity is determined by the motion (flow or creep) of vortices drawn by the Lorentz force  $\mathbf{F} = (\phi_0/c) [\mathbf{B} \times \mathbf{j}]$ . In a superconducting state the resistivity  $\rho$  is a strong (exponential) function of the activation energy:  $\rho \approx \rho_n(B/B_{c2}) \exp(-U/kT)$ ,<sup>11</sup> whereas  $U$  is in turn a nonlinear function of  $j$  and  $B$ . This leads to a prominent redistribution of  $j$  over the sample (the total current  $I$  is kept constant). Moreover, if the surface barriers are effective, then a certain part  $I_{edge}$  of  $I$  flows along the edges of the sample, giving rise to additional current and potential redistribution. Note that in the flux flow regime ( $U_{bulk} = 0$ ) and absence of surface barriers ( $I_{edge} = 0$ ) the effect of redistribution disappears, since  $\rho$  is just renormalized in the whole sample by a constant factor with respect to its normal value:  $\rho \approx \rho_n B/B_{c2}$ ,<sup>12</sup> which does not affect the current density  $j$  provided  $I = \text{const}$ . In this case the potential  $\varphi$  is renormalized

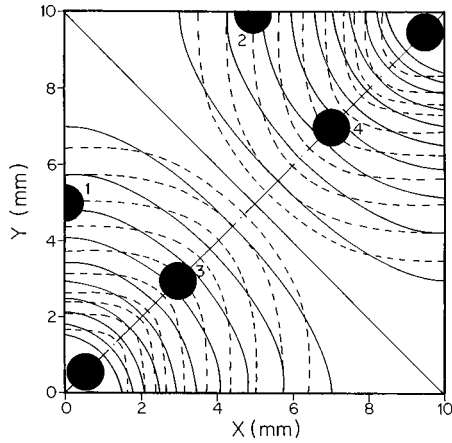


FIG. 1. Square sample (side  $w=10$  mm) with current and voltage contacts shown as black circles. Current contacts are located at the corners  $(0,0)$  and  $(w,w)$ . The ‘‘edge’’ voltage contacts  $V_1$  and  $V_2$  are attached to the middles of the sample edges, and the ‘‘bulk’’ contacts  $V_3$  and  $V_4$  are located in the same diagonal with the current ones at  $(0.3w,0.3w)$  and  $(0.7w,0.7w)$ . The diameter of the circles corresponds to the real size of the contacts. The solid and dashed curves show the equipotential contours ( $\varphi=\text{const}$ ) in the normal ( $\mu=0$ ) and superconducting ( $\mu=2$ ) states, respectively, obtained by numerical simulation.

by the same factor  $B/B_{c2}$ , thus the ratio of potentials taken at arbitrary points of the sample remains the same as in the normal state. In other words, the redistribution of  $j$  and change in ratios of voltages is determined by the  $U(j)$  dependence and by the efficiency of surface barriers. Generally speaking,  $U$  depends on  $B$  as well, but in our case  $B$  is almost homogeneous over the sample since the self-fields induced by  $I$  are much less than the external magnetic field. Such a redistribution of  $j$  provides as a useful tool to study the  $U(B,j)$  dependence in various regimes of flux creep<sup>8–10</sup> and of the interplay between the bulk pinning and surface barriers.

## II. EXPERIMENT

The sample is the  $\text{YBa}_2\text{Cu}_3\text{O}_7$  film of the width  $d=2000$  Å grown by laser ablation on  $\text{SrTiO}_3$  substrate with  $c$  axis perpendicular to the film. The  $ab$  dimensions are  $10\times 10$  mm. The film is thermally sunk to a copper block that has platinum and GaAs thermometers. This sample housing is mounted in a variable temperature cryostat (closed cycle cryogenic refrigerator system LTS-22). The temperature is regulated by digital temperature controller Lake Shore 330 with stability better than 0.02 K.

Indium contact pads of 1 mm in diameter are made by pressing indium into the film. Silver wires of 20  $\mu\text{m}$  diameter were attached to indium pads either with silver paste or by pressing it in indium pads. The contact resistance is approximately 1–5  $\Omega$ . Two current contacts are attached at the corners of the sample along one of the diagonals, i.e., at the points  $(0,0)$  and  $(w,w)$ , where the axes  $x$  and  $y$  are chosen as shown in Fig. 1 and  $w=10$  mm is the side of the square sample. The total current  $I=100$   $\mu\text{A}$  flowing through these contacts is kept constant. One pair of voltage contacts, No. 1 and No. 2, which we refer to as ‘‘edge contacts,’’ are located

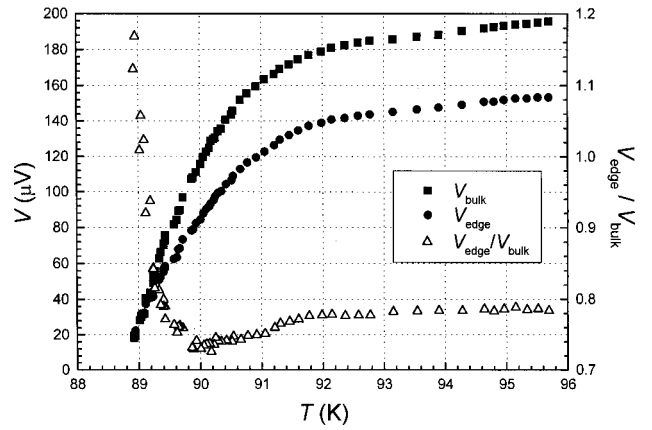


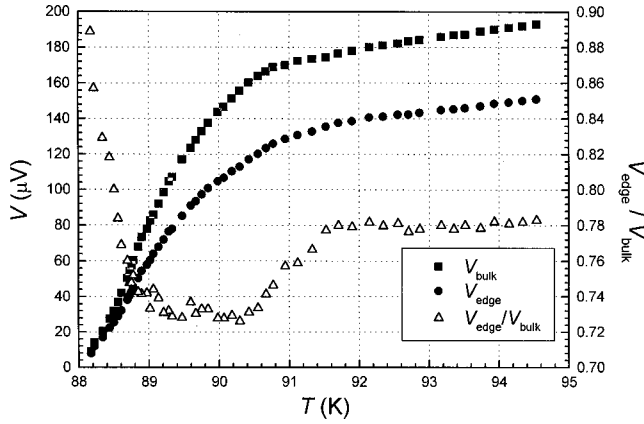
FIG. 2. Experimentally measured voltages  $V_{edge}=V_1-V_2$ ,  $V_{bulk}=V_3-V_4$ , and their ratio  $\delta=V_{edge}/V_{bulk}$  as functions of temperature at  $B=0.2$  T.

at  $(0,0.5w)$  and  $(0.5w,w)$ , i.e., in the middles of the sample edges. Another pair, No. 3 and No. 4, which we refer to as ‘‘bulk contacts,’’ are located approximately at  $(0.3w,0.3w)$  and  $(0.7w,0.7w)$  at the same diagonal with the current contacts.

The data were taken by the use of both ac and dc methods. We measure voltage on two couples of potential contacts simultaneously at the different values of temperature and magnetic field. Two lock-in amplifiers SR 830 were used for measuring of the voltage by the ac method. The internal oscillator of one of them was the current source for measuring circuit and the source of reference voltage for both lock-in amplifiers. In the dc method we used programmed current source Keithley 220 and digital nanovoltmeter Keithley 182. We use the field-cooled scheme (i.e., the magnetic field is almost homogeneous inside the film) with  $0.1 < B < 0.6$  T. The upper boundary is due to our device limitations, the lower one was chosen to ensure that the self fields of the measuring current  $I$  are much less (by factor of 100 at least) than  $B$ .

## III. RESULTS AND DISCUSSION

In Fig. 2 we show the voltages  $V_{edge}=V_1-V_2$  and  $V_{bulk}=V_3-V_4$ , measured at the edge and at the bulk pairs of contacts, respectively, as functions of temperature at  $B=0.2$  T, together with the ratio  $\delta=V_{edge}/V_{bulk}$ . The superconducting transition starts at  $T_c(B=0.2\text{ T})\approx 92$  K and has a width of approximately 3 K. The same quantities are shown in Fig. 3 at  $B=0.6$  T with  $T_c(B=0.6\text{ T})\approx 91$  K. The most interesting feature is the variation of  $\delta$  vs temperature and field or, generally speaking, along the transition from a normal to a superconducting state. In the normal state (at  $T > T_c$ ) we get  $\delta_n \approx 0.78$  independently on  $B$ . As temperature drops down below  $T_c$  the ratio at first slightly decreases but then sharply increases up to  $\delta \approx 1.1-1.2$  at  $B=0.2$  T (Fig. 2) and  $\delta \approx 0.9$  at  $B=0.6$  T (Fig. 3). We obtain similar results in the cases where the superconducting transition is induced by decreasing  $B$  at constant temperature  $T=89.1$  K (see Fig. 4). Here  $\delta$  changes from  $\delta_n \approx 0.78$  for  $B=0.6$  T (where  $V_{bulk}(89.1\text{ K})/V_{bulk}(T_c) \approx 0.5$ , see Fig. 3), which corresponds to almost normal state, up to  $\delta \approx 1.2$  for  $B=0.2$  T (where  $V_{bulk}(89.1\text{ K})/V_{bulk}(T_c) \approx 0.15$ , see Fig. 2),

FIG. 3. The same as in Fig. 2, but at  $B=0.6$  T.

which corresponds to superconducting state.

As has been discussed above, the variation of  $\delta$  as the sample undergoes a superconducting transition, should be explained by either non-Ohmic behavior of the bulk resistivity  $\rho = \rho(j)$  or by effect of surface barriers. The resistivity is determined by the moving vortex liquid, since throughout all the measurement we are very close to  $T_c$  and definitely in the vortex liquid regime.<sup>8</sup> The dependencies of  $V_{bulk}$  and  $V_{edge}$  on the  $I$  (not the current density  $j$ ) at  $T=89.1$  K are shown in Fig. 5. The linear (Ohmic) part  $V(I)$ , which corresponds to the unpinned vortex liquid,<sup>8</sup> starts above  $I_{pin} \approx 50 \mu A$ , whereas the low current part  $I < I_{pin}$  (see inset to Fig. 5) corresponds to pinned vortex liquid with strongly nonlinear  $\rho(I)$ . Since our transport current  $I=100 \mu A$  does not significantly exceed  $I_{pin}$ , most of the sample (especially the parts with  $j$  lower than the average  $\langle j \rangle$  over the sample, i.e., apart from the main diagonal) is characterized by a strong dependence  $\rho(j)$  in the superconducting state. This justifies the change of the current distribution in the sample if compared to the normal state.

In order to compare the observed behavior of  $\delta$  with the theoretical prediction we analyzed the problem numerically using the  $48 \times 48$  point square matrix. The two-dimensional Laplace equation  $\Delta \varphi = 0$  for the electrostatic potential  $\varphi(x, y)$  was solved by the relaxation method. For the non-Ohmic behavior of  $\rho$  we used the model where

$$\rho(j) = \rho_0 (j/j_c)^\mu, \quad (1)$$

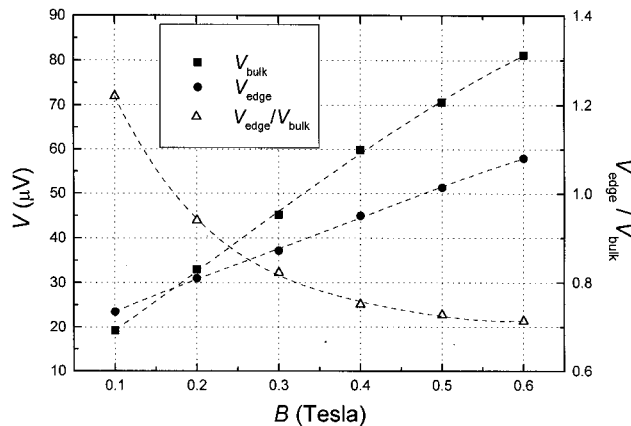
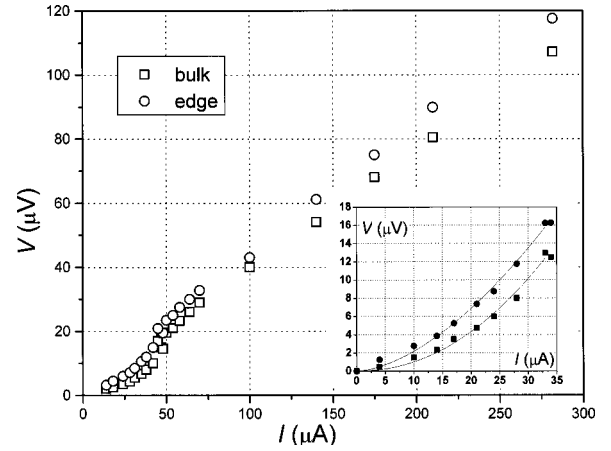
FIG. 4. Voltages  $V_{edge}$ ,  $V_{bulk}$  and their ratio  $\delta = V_{edge}/V_{bulk}$  as functions of field at  $T=89.1$  K.

FIG. 5. Experimentally measured  $V_{edge}$  and  $V_{bulk}$  as functions of the total current  $I$ . Above  $I_{pin} \approx 50 \mu A$  the dependence is almost linear (unpinned vortex liquid), whereas below  $I_{pin}$  one gets a non-Ohmic dependence (pinned vortex liquid), shown in greater detail in the inset. The nonlinear part is fitted by  $V \propto I^{\mu+1}$ , which corresponds to Eq. (1) (see values of  $\mu$  and discussion in the text).

which corresponds to the general case  $\rho(j) = \rho_0 \exp[-U(j)/kT]$  if one assumes  $U(j) = U_0 \ln(j_c/j)$  (Ref. 13) with  $\mu = U_0/kT$ . The normal metal, where  $\rho = \rho_0 = \text{const}$ , corresponds to  $\mu = 0$ . Obviously  $\delta$  appears to be a function of  $\mu$  only and depends neither on  $\rho_0$  nor on  $j_c$  since varying these parameters one gets a corresponding change of the voltages (but not their ratios) in the whole sample. For the same reason  $\delta$  does not depend on the total current  $I$  flowing through the sample provided  $I_{edge} = 0$ .

In Fig. 1 we show the results of the numerical solution of the Laplace equation. The solid and dashed curves show the equipotential contours  $\varphi = \text{const}$  for a normal metal ( $\mu = 0$ ) and for a superconductor (as an example, we chose  $\mu = 2$ ), respectively. The numerically obtained  $\delta_n = 0.77$  in the normal state (provided the voltages are measured between the centers of contacts  $V_1-V_2$  and  $V_3-V_4$  shown in Fig. 1) is in complete agreement with the experimental data, especially taking into account that the real size of contacts is about  $1 \text{ mm} \approx 0.1 w$ . The equipotential contours become more convex in the superconducting state, and their convexity grows with increasing  $\mu$ . This means that the current  $j$  which flows perpendicularly to the equipotential contours, acquires more fanlike structure and fills in the ‘‘side corners’’  $(0, w)$  and  $(w, 0)$  of the sample (see Fig. 6). This also means that  $\delta$  should decrease with increasing  $\mu$ . The dependence of  $\delta$  on  $\mu$  obtained by numerical simulations is shown in Fig. 7.

Experimentally we observe a slight drop of  $\delta$  with decreasing temperature (see Figs. 2 and 3), followed by a relatively sharp increase of  $\delta$  above the ‘‘normal’’ value  $\delta_n$ . The slight decrease of  $\delta$  agrees with continuous destroying of the Ohmic behavior as the sample becomes superconducting. In other words, as temperature decreases the effective  $\mu$  grows from the normal state value  $\mu = 0$ , and  $\delta$  drops correspondingly. For  $B = 0.6$  T (see Fig. 3)  $\delta$  drops down to  $\delta \approx 0.72$ , which, according to Fig. 7, corresponds to  $\mu \approx 0.2$ . Such a behavior is consistent with the above discussion. It is worth mentioning that this method of finding of  $\mu$  is self-consistent and much better than any estimations obtained directly from the current-voltage curve (see inset to Fig. 5). The data in the

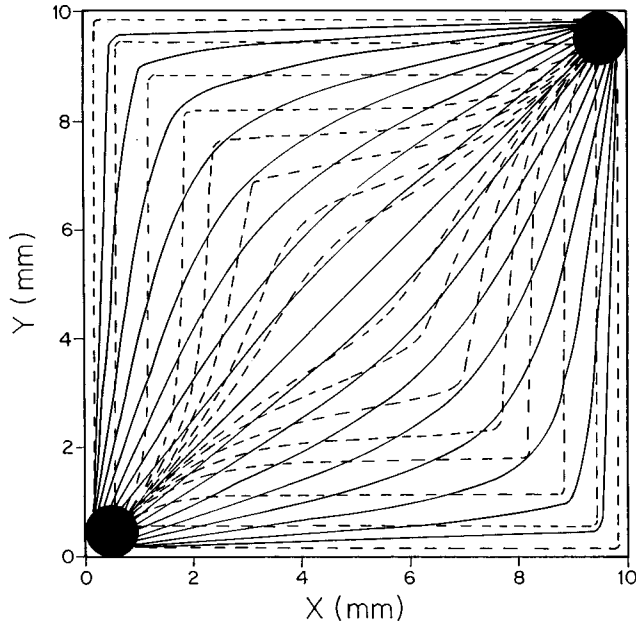


FIG. 6. Current lines in the normal ( $\mu=0$ ) and superconducting ( $\mu=2$ ) state, shown by solid and dashed lines, respectively, obtained by numerical simulation (compare with Fig. 1).

inset are fitted as  $V \propto I^{\mu+1}$ , which corresponds to Eq. (1). The latter estimation provides mutually conflicting values:  $\mu \approx 0.6$  for  $V_{edge}$  and  $\mu \approx 1.1$  for  $V_{bulk}$  which both disagree with above estimation  $\mu \approx 0.2$ . This just confirms that in our geometry, where the current density  $j$  is not constant, the exponent  $\mu$  cannot be obtained directly from  $I$ - $V$  curves (where  $I$  is the total current) and our method of determination of  $\mu$  via  $\delta$  should be applied.

However, the sharp growth of  $\delta$  observed at a further decrease of  $T$  (see Figs. 2 and 3) cannot be explained by the non-Ohmic dependence, where  $\rho$  increases with  $j$ . Such a behavior of  $\delta$  can be explained by the effect of a surface barrier which prevents vortices from entering and exiting the sample and gives rise to a surface current  $I_{edge}$ . The latter flows along the sample edge in the  $\lambda$  layer, where  $\lambda$  is the London penetration depth. Thus for each cross section of the sample one gets  $I = I_{edge} + I_{bulk}$  with  $I_{bulk} = \int j ds$  (see Fig. 8). The values of  $I_{edge}$  and  $j$  should be found from the con-

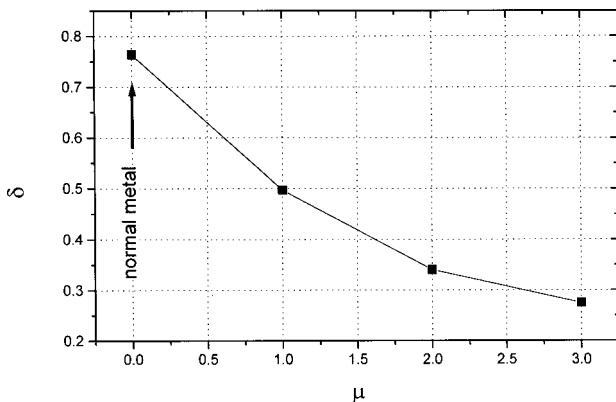


FIG. 7. Numerically obtained  $\delta = V_{edge}/V_{bulk}$  as a function of  $\mu$  in the absence of surface barriers ( $I_{edge}=0$ ). Note that  $\mu=0$  corresponds to the normal state.

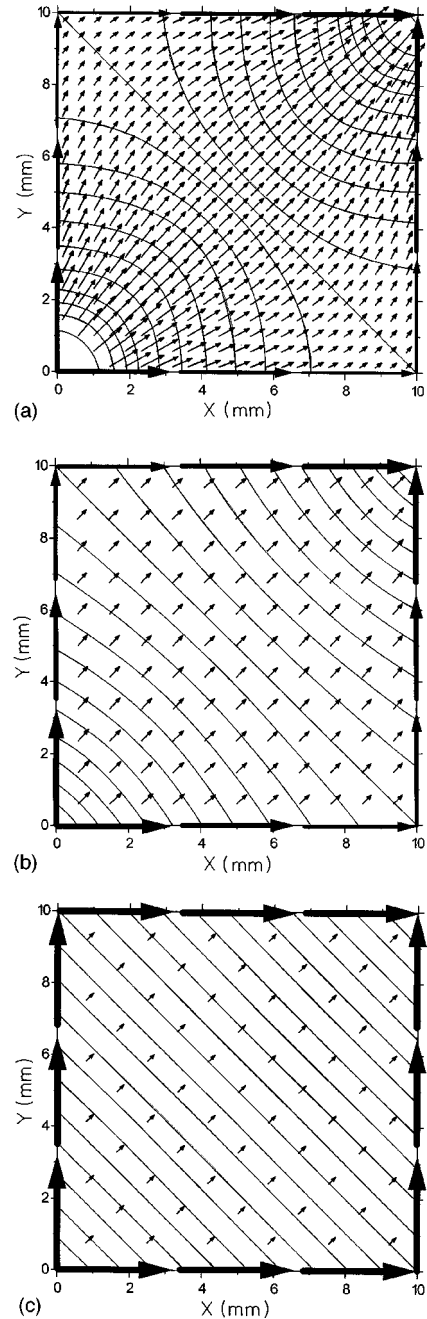


FIG. 8. Numerically obtained current lines in a superconductor ( $\mu=2$ ) with surface barrier of different strength: (a) weak ( $s=0.25$ ), (b) moderate ( $s=2$ ), (c) strong ( $s=18$ ). The lines show the equipotential contours  $\varphi = \text{const}$ . The large edge arrows illustrate (by their width)  $I_{edge}$ , which is maximal at the current contacts and gradually decreases towards the other two corners. The small arrows illustrate (by their density and length) the current density  $j$  in the bulk. As  $s$  grows,  $I_{edge}$  increases and  $I_{bulk} = I - I_{edge}$  decreases. In the case of very strong barrier ( $s \gg 1$ ) most of  $I$  flows along the edges:  $I_{edge} \gg I_{bulk}$ , thus  $I_{edge} \approx I$ , the potential  $\varphi$  changes almost linearly along the perimeter of the sample, and the lines  $\varphi = \text{const}$  become approximately straight.

dition of continuity of vortex flow (or the same, of the electric field  $E$ ) as discussed in Ref. 4, where the case of a simpler (slab) geometry was considered. The strength of the surface barrier can be described by the ratio  $I_{edge}/I_{bulk}$ , which in turn depends on the interplay between the activa-

tion energies  $U_{edge}$  at the surface (edge) and  $U_{bulk}$  in the bulk.<sup>4</sup> In our geometry, however,  $I_{edge}$  and  $I_{bulk}$  vary with the chosen cross section of the sample (see Fig. 8). The edge current  $I_{edge}$  gets maximum at the current contacts  $(0,0)$ - $(w,w)$  and decreases continuously towards the corners  $(0,w)$ - $(w,0)$ . The bulk current  $I_{bulk} = I - I_{edge}$  changes correspondingly. Thus we choose the parameter  $s = I_{edge}^{\min}/I_{bulk}^{\max}$  for characterization of the surface barrier efficiency in our geometry. Here  $I_{edge}^{\min}$  and  $I_{bulk}^{\max}$  correspond to the diagonal cross section through the corners  $(0,w)$  and  $(w,0)$ . Figure 8 illustrates the numerically obtained  $I_{edge}$  and  $j$  (shown as arrows) together with equipotential contours  $\varphi = \text{const}$  (which are mutually perpendicular with the current lines) for  $\mu = 2$  and different values of  $s$ . For a very strong surface barrier ( $s \gg 1$ ) we get  $I_{edge} \approx I = \text{const}$ , thus  $\varphi$  changes almost linearly along the perimeter of the sample [see Fig. 8(c)]. In this case  $j$  is small ( $I_{bulk} \ll I_{edge}$ ), approximately uniform, and parallel to the main diagonal irrespective of the particular dependence of  $\rho$  on  $j$ . Therefore the equipotential contours are also almost straight and perpendicular to  $j$ . The numerical study provides  $\delta = 1.18$  for the case of “infinite” surface barrier (i.e., for  $s \rightarrow \infty$ ) and our contact geometry (see Fig. 1). This is consistent with the maximal value obtained for  $\delta$  in the experiment (see Fig. 2).

We see that in the geometry of our experiment the effects of non-Ohmic resistance (growth of  $\rho$  with  $j$ ) and of the surface barrier on  $\delta$  are opposite and thus competing. The fact that non-Ohmic behavior dominates at the earliest stages of the transition [ $\rho/\rho(T_c) \approx 1$ ], whereas the surface barrier becomes effective provided most of the sample is already superconducting [ $\rho/\rho(T_c) \approx 0.1$ ], is quite natural. The presence of even a small fraction of superconducting (non-Ohmic) phase in the bulk should result in a redistribution of

$j$  in the sample, leading to a decrease of  $\delta$ . However, the efficiency of the surface barrier implies that most of the sample edge should be superconducting, otherwise the vortices can easily enter and leave the sample through the normal segments of the edge. Thus at the first stages of the superconducting transition when most of the edge is still normal, we expect no effect of the surface barrier.

#### IV. CONCLUSION

We have shown experimentally and theoretically that the nonuniform current distribution in superconductors is strongly affected by both the type of dependence of  $\rho$  on  $j$  and by the presence of a surface barrier. In the geometry of our experiment the above two effects on the potential ratio  $\delta$  are opposite and compete with each other. At the first stage of the superconducting transition, where a lesser part of the (inhomogeneous) sample becomes superconducting and most of the edge is normal, the surface barrier is not effective and  $\delta$  decreases with respect to  $\delta_n$ . As most of the sample and, correspondingly, most of its edge become superconducting, the surface barrier starts to dominate, giving rise to an increase of  $\delta$ . The proposed method enables various modifications (different sample geometries, location of contacts, etc.) and provides a useful tool for the study of bulk and surface pinning as well as their interplay.

#### ACKNOWLEDGMENTS

We acknowledge support by the German-Israeli Foundation (GIF) and by the Israel Academy of Sciences. We are grateful to J. Kraftmakher, G. Citver, A. Butenko, and M. Tsindlekht for help in the experiments.

<sup>1</sup>V. N. Kopylov, A. E. Koshelev, I. F. Schegolev, and T. G. Togonidze, *Physica C* **170**, 291 (1990); M. Konczykowski, L. Burlachkov, Y. Yeshurun, and F. Holtzberg, *Phys. Rev. B* **43**, 13 707 (1991); D.-X. Chen and A. Sanchez, *ibid.* **45**, 10 793 (1991); *Cryogenics* **33**, 695 (1993); N. Chikumoto, M. Konczykowski, N. Motohira, and A. P. Malozemoff, *Phys. Rev. Lett.* **69**, 1260 (1992); F. Zuo, D. Vacaru, H. M. Duan, and A. M. Hermann, *Phys. Rev. B* **47**, 5535 (1993); C. J. van der Beek, B. Schmidt, M. Konczykowski, V. M. Vinokur, and G. W. Crabtree, *Physica C* **235-240**, 2813 (1994); D. Majer, E. Zeldov, M. Konczykowski, V. B. Geshkenbein, A. I. Larkin, L. Burlachkov, V. M. Vinokur, and N. Chikumoto, *ibid.* **235-240**, 2765 (1994); Yang Ren Sun, J. R. Thompson, H. R. Kerchner, D. K. Christen, M. Paranthaman, and J. Brynstad, *Phys. Rev. B* **50**, 3330 (1994); Yang Ren Sun, J. R. Thompson, J. Schwartz, D. K. Christen, Y. C. Kim, and M. Paranthaman, *ibid.* **51**, 581 (1995); J. A. Lewis, V. M. Vinokur, J. Wagner, and D. Hinks, *ibid.* **52**, R3852 (1995); M. Reissner, *Physica C* (to be published).

<sup>2</sup>W. R. White, A. Kapitulnik, and M. R. Beasley, *Phys. Rev. Lett.* **70**, 670 (1993); Dan T. Fuchs, E. Zeldov, M. Rappaport, T. Tamegai, S. Ooi, and H. Shtrikman, *Nature (London)* **391**, 373 (1998).

<sup>3</sup>A. E. Koshelev, *Physica C* **191**, 219 (1992); L. Burlachkov, *Phys.*

*Rev. B* **47**, 8056 (1993); R. G. Mints and I. B. Snapiro, *ibid.* **47**, 3273 (1993); L. Burlachkov, V. B. Geshkenbein, A. E. Koshelev, A. I. Larkin, and V. M. Vinokur, *ibid.* **50**, 16 770 (1994); A. E. Koshelev, *Physica C* **223**, 276 (1994); K. I. Kugel and A. L. Rakhmanov, *ibid.* **251**, 307 (1995); E. H. Brandt, R. G. Mints, and I. B. Snapiro, *Phys. Rev. Lett.* **76**, 827 (1996); F. Bass, V. D. Freilikher, B. Ya. Shapiro, and M. Shvartsner, *Physica C* **260**, 231 (1996).

<sup>4</sup>L. Burlachkov, A. E. Koshelev, and V. M. Vinokur, *Phys. Rev. B* **54**, 6750 (1996).

<sup>5</sup>C. P. Bean and J. D. Livingston, *Phys. Rev. Lett.* **12**, 14 (1964).

<sup>6</sup>E. Zeldov, A. I. Larkin, V. B. Geshkenbein, M. Konczykowski, D. Majer, B. Khaykovich, V. M. Vinokur, and H. Shtrikman, *Phys. Rev. Lett.* **73**, 1428 (1994).

<sup>7</sup>M. V. Feigel'man, V. B. Geshkenbein, A. I. Larkin, and V. M. Vinokur, *Phys. Rev. Lett.* **63**, 2303 (1989).

<sup>8</sup>G. Blatter, M. V. Feigel'man, V. B. Geshkenbein, A. I. Larkin, and V. M. Vinokur, *Rev. Mod. Phys.* **66**, 1125 (1994).

<sup>9</sup>Y. Yeshurun, A. Shaulov, and A. P. Malozemoff, *Rev. Mod. Phys.* **68**, 911 (1996).

<sup>10</sup>E. H. Brandt, *Rep. Prog. Phys.* **58**, 1465 (1995).

<sup>11</sup>M. R. Beasley, R. Labusch, and W. W. Webb, *Phys. Rev.* **181**, 682 (1969).

<sup>12</sup>J. Bardeen and M. J. Stephen, Phys. Rev. A **140**, 1197 (1965); see also M. Tinkham, *Introduction to Superconductivity* (McGraw-Hill, New York, 1975).

<sup>13</sup>E. Zeldov, N. M. Amer, G. Koren, A. Gupta, R. J. Gambino, and

M. W. McElfresh, Phys. Rev. Lett. **62**, 3093 (1989); Appl. Phys. Lett. **56**, 680 (1990); Y. Abulafia, A. Shaulov, Y. Wolfus, R. Prozorov, L. Burlachkov, Y. Yeshurun, D. Majer, E. Zeldov, and V. M. Vinokur, Phys. Rev. Lett. **75**, 2404 (1995).